

Comparative study of sunset yellow dye adsorption onto cornelian cherry stones-based activated carbon and carbon nanotubes

F. O. Erdogan*

Department of Chemistry and Chemical Processing Technologies, Kocaeli Vocational School, Kocaeli University,
41140, Kocaeli, Turkey

Received, December 13, 2017; Accepted, July 20, 2018

The objective of the study was to prepare low-cost activated carbon from cornelian cherry stones (*Cornus mas* L.) and compare its adsorption behavior for a food dye with that of commercial multiwalled carbon nanotubes. The cornelian cherry stones activated carbon (AC) and commercial multi-walled carbon nanotubes (MWCNT) were characterized by N₂ adsorption isotherms and SEM (scanning electron microscopy). Adsorption of a food dye, sunset yellow FCF, by AC and MWCNT was examined in detail. Batch adsorption test showed that the extent of sunset yellow adsorption was dependent on dye concentration, contact time, solution temperature and adsorbent dosage. The experimental adsorption equilibrium data were compared to the Langmuir, Freundlich, Temkin and DR isotherm models and the isotherm model parameters were determined. The maximum adsorption capacity was found to be 125.3 and 43.8 mg/g for AC and MWCNT, respectively. Pseudo-first-order, pseudo-second-order and Elovich equations were fitted to the kinetic data, and the rate constants were evaluated. Thermodynamic parameters enthalpy, entropy and Gibbs free energy changes were established. Results showed that activated carbon produced from cornelian cherry stones is suitable for the adsorption of sunset yellow food dye and could be used as a low-cost effective adsorbent in the treatment of industrial wastewater.

Keywords: Cornelian cherry stones, Adsorption isotherms, LiOH activations, Sunset yellow, Multiwalled carbon nanotubes.

INTRODUCTION

Activated carbon is one of the widely used adsorbents in removal of dyes because of its large surface area, favorable pore size distribution and high adsorption capacities. Activated carbon is produced from a variety of carbonaceous raw materials such as cherry stones, apricot seed kernels, almond shells, peach stones, orange peels, pistachio shells, coal, petroleum coke, lignite, wood, resin, coconut husks, tomato stems, olive stones, waste tires, waste paper, fish waste [1-16]. The surface properties and adsorption characteristics of activated carbons depend on the physical and chemical properties of the raw materials and the activation methods. Activated carbons can be produced by physical or chemical activation. Chemical activation, is a single-step method of preparation of the raw material in the presence of chemical agents such as ZnCl₂, AlCl₃, LiOH, KOH, NaOH, K₂CO₃, Na₂CO₃, H₃PO₄ and H₂SO₄ [17-22]. Many studies have been reported for activated carbon production using various raw materials and activation agents. Philip [16] produced activated carbon from apricot stones by activation with H₃PO₄. The highest specific surface area, micropore volume and mean pore radius were found as 1603 m² g⁻¹, 0.752 cm³ g⁻¹ and 9.4 Å,

respectively. Fu *et al.* [9] produced activated carbon from tomato stems at different carbonization temperatures (500, 600, 650, 700, 750 and 800 °C) and impregnation ratios (1, 1.5, 2, 2.5 and 3). In this study, BET surface area, micropore area, total volume, and micropore volume of activated carbon obtained at 700 °C with impregnation ratio of 2.5 were 971 m² g⁻¹, 838 m² g⁻¹, 0.576 cm³ g⁻¹ and 0.425 cm³ g⁻¹, respectively. Tian *et al.* [23] produced activated carbon from cotton stalk with KOH and investigated the effects of micropore development on the physicochemical properties of the activated carbons. Al-Rahbi and Williams [24] produced activated carbon from waste tyres with alkali chemical reagents (KOH, K₂CO₃, NaOH, and Na₂CO₃). The maximum surface areas obtained by chemical activation with KOH, K₂CO₃, NaOH, and Na₂CO₃ were 621, 133, 128 and 92 m² g⁻¹, respectively. To the best of our knowledge, no study has been reported on the preparation of activated carbon from cornelian cherry stones by chemical activation with LiOH.

Carbon nanotubes are newly emerged carbonaceous materials, their characteristic structures and electronic properties make them interact strongly with dyes, *via* non-covalent forces such as hydrogen bonding, van der Waals forces and hydrophobic interactions [25]. Carbon

*To whom all correspondence should be sent:

E-mail: foerdogan@gmail.com

F. O. Erdogan: Comparative study of sunset yellow dye adsorption onto cornelian cherry stones-based activated carbon and ...
 nanotubes with different diameters would have different surface area, which would affect their adsorptive properties [26].

Dyes (synthetic organic substances) are widely used in food, textile, leather, paper, cosmetic, pharmaceutic and automotive industries. Sunset yellow (SY) is a pyrazolone dye used in food products such as beverages, candies, dairy, pharmaceuticals and bakery products [27, 28]. Many methods have been employed to remove dyes from aqueous solution, and adsorption is considered superior to the other techniques.

The main objects of this study are: (i) to study the feasibility of using the activated carbon produced from cornelian cherry stones as a low-cost adsorbent for the removal of sunset yellow (SY) dye; (ii) to compare its adsorption behavior for the food dye to that of commercial multiwalled carbon nanotubes (MWCNT); (iii) to determine the various parameters affecting sorption, such as contact time, amount of adsorbents and temperature of the solution; (iv) to determine the applicability of various isotherm models ((i.e., Langmuir, Freundlich, Temkin and DR) to find out the best-fit isotherm equation; and (v) to determine thermodynamic and kinetic parameters and explain the nature of the adsorption.

MATERIALS AND METHODS

Materials

In this study, cornelian cherry stones were obtained from Havza in Samsun province in Turkey. The precursor, cornelian cherry stones were first air dried, then crushed and sieved in order to get standardized particle dimensions. Then, cornelian cherry stones were contacted with a dilute 10 vol.% sulfuric acid solution for 8 h (sulfuric acid contributes to the removal of inorganic components from lignocellulosic materials) and washed with hot distilled water. Multiwalled carbon nanotubes were provided by CNT CO., LTD (Korea) [44].

Preparation of the activated carbons

10 g of dried cornelian cherry stones (<2 mm) were mixed in a beaker with 200 mL of LiOH solution which corresponded to an impregnation ratio of 4:1 (weight of impregnation reagent/weight of cornelian cherry stones) for 8 h at 65 °C. The impregnated sample was then dried overnight in a moisture oven at 120 °C. Then, the impregnated sample was carbonized in a tube furnace (Protherm STF) under N₂ flow at a heating rate of 10 °C/min up to 700 °C for 1 h. After the activation the sample was allowed to cool down to room temperature under N₂ flow before its removal from the furnace.

The activated sample was washed several times with HCl and hot distilled water to remove residual chemicals until gave no chloride reaction with AgNO₃. The activated sample was dried for about 6 h at a temperature of 120 °C. Activated sample was stored in a sealed flask and labelled. The pores of activated carbon were characterized by analysis of N₂ adsorption-desorption isotherms at 77 K using Micromeritics TriStar II 3020.

Adsorbate

The commercial food dye sunset yellow FCF (C₁₆H₁₀N₂Na₂O₇S₂, molecular weight 452.37 g/mol, C.I. 15985, λ_{max}=482 nm, chemical structure shown in Figure 1) was supplied by Sigma-Aldrich. Distilled water was used to prepare all solutions.

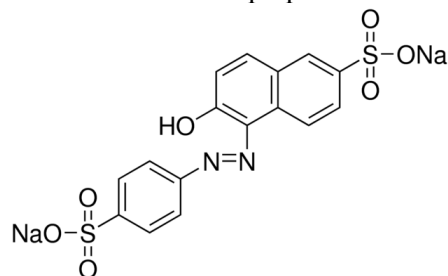


Figure 1. Chemical structure of sunset yellow FCF.

Adsorption equilibrium studies

Adsorption of SY on cornelian cherry stones-based activated carbon (AC) and MWCNT was studied by batch experiments. Equilibrium adsorption studies were conducted in a set of 60 mL capped volumetric flasks containing different amounts of adsorbent in the range of 0.05-0.09 g/L for AC and 0.01-0.03 g/L for MWCNT, 50 mL initial concentrations of SY solutions (10-50 mg/L for AC, 10-100 mg/L for MWCNT). Flasks were shaken in a mechanical shaker (GFL 1086) at 100 rpm and different temperatures (30, 40 and 50°C). After adsorption, samples were filtered and then the concentrations of SY in the supernatant solution were analyzed. All concentrations were measured on a UV spectrophotometer (LaboMed Inc.) at 482 nm. The adsorption efficiency (E) was calculated using equation (1):

$$E = \frac{(C_0 - C_e)}{C_0} 100 \quad (1)$$

where C₀ and C_e (mg/L) are the initial and equilibrium liquid-phase concentrations of dye, respectively. The SY uptake at equilibrium (q_e (mg/g)), was calculated using equation (2):

$$q_e = \frac{(C_0 - C_e)V}{W} \quad (2)$$

where V (L) is the volume of the solution, and W

F. O. Erdogan: Comparative study of sunset yellow dye adsorption onto cornelian cherry stones-based activated carbon and ...
 (g) is the mass of the adsorbent used in the experiments. The equilibrium data were simulated using the Freundlich, Langmuir, Temkin and DR isotherm models [27].

Adsorption kinetics

Kinetic adsorption experiments were carried out by adding 0.05 g/L of AC or 0.01 g/L of MWCNT to 50 mL of 10 mg/L SY dye aqueous solutions at temperatures of 30, 40 and 50°C. The uptake of SY at time t , q_t (mg/g) was calculated by the following equation:

$$q_t = \frac{(C_0 - C_t)V}{W} \quad (3)$$

where C_t (mg/L) is the liquid-phase concentration of dye at time t , (min).

In order to predict the adsorption behavior of sunset yellow FCF on the adsorbents, pseudo-first-order and pseudo-second-order kinetic equations, which are described with equations (4) and (5), respectively, were applied for modeling experimental data:

$$\log(q_e - q_t) = \log q_e - \frac{k_1 t}{2.303} \quad (4)$$

$$\frac{t}{q_t} = \frac{1}{k_2 q_e^2} + \frac{t}{q_e} \quad (5)$$

where k_1 (1/min) and k_2 (g/mg min) are the adsorption rate constants of the pseudo-first-order and pseudo-second-order, respectively [27, 29]. Elovich equation has been generalized and frequently used in the adsorption studies of many pollutants in aqueous solution:

$$q_t = \left(\frac{1}{\beta} \right) \ln(\alpha\beta) + \left(\frac{1}{\beta} \right) \ln t \quad (6)$$

where α is the chemisorption rate (mg/g min) and β is a coefficient related with the extension of covered surface and activation energy of chemisorption (g/mg). The equation constants can be determined by plotting the straight line of q_t versus $\ln t$ [30].

Adsorption thermodynamics

The rate constant (pseudo-first or pseudo-second order) of dye adsorption is expressed as a function of the temperature by the Arrhenius relationship [31,32]:

$$\ln k = \ln A - \left(\frac{E_a}{R} \right) \frac{1}{T} \quad (7)$$

where E_a is the Arrhenius activation energy (kJ/mol), A is the Arrhenius factor, R is the molar gas constant (8.314 J/mol K) and T is the absolute

temperature (K).

To describe the thermodynamic behavior of the adsorption of SY dye onto AC or MWCNT, the thermodynamic parameters including the changes in free energy (ΔG°), enthalpy (ΔH°) and entropy (ΔS°) were calculated by the following equations:

$$\Delta G^\circ = -RT \ln K_c \quad (8)$$

$$\ln K_c = -\frac{\Delta H^\circ}{RT} + \frac{\Delta S^\circ}{R} \quad (9)$$

where R is the universal gas constant (8.314 J/mol K), T is the temperature (K) and $K_c = C_{ads}/C_e$ is the equilibrium constant of the SY adsorption equilibrium (which is a ratio of C_{ads} , the SY concentration in the adsorbent, and C_e , the SY concentration in the adsorbate [29]).

RESULTS AND DISCUSSION

Characterization of the carbonaceous materials

The surface physical properties of the adsorbents were characterized with an automated gas sorption apparatus using N_2 as adsorbate at 77.4 K. Nitrogen adsorption is a standard technique widely used for the determination of porosity of adsorbents. Figures 2 and 3 show the isotherms of the LiOH treated sample (AC) and MWCNT, respectively. Appearance of hysteresis loop indicates the presence of mesopores. The pore structure of the adsorbents was calculated by using the t-method analysis from the adsorption branch of the nitrogen isotherms [9, 27].

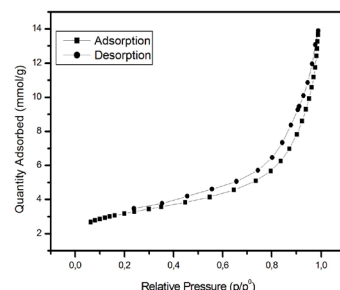


Figure 2. Adsorption-desorption isotherms of AC.

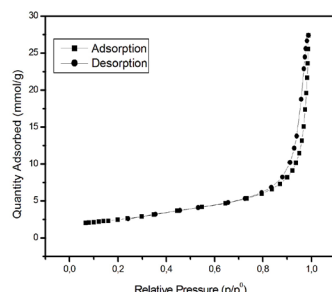


Figure 3. Adsorption-desorption isotherms of MWCNT.

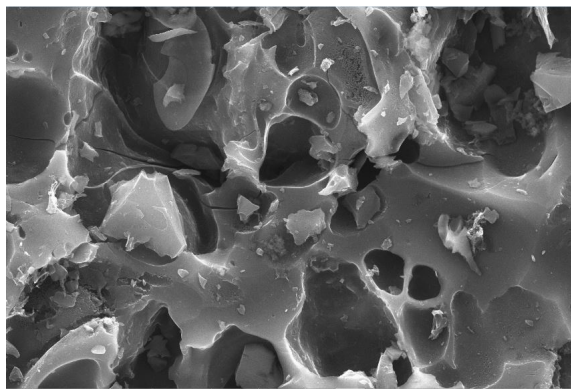
Table 1. Textural parameters of the adsorbents.

Properties	AC	MWCNT
BET surface area (m^2/g)	249.5	193.7
Langmuir surface area (m^2/g)	337.3	265.2
Total pore volume (mL/g)	0.445	0.250
Micropore volume (mL/g)	0.039	0.062
Average pore width (nm)	7.14	15.51

Table 1 shows the BET and Langmuir surface areas, total pore volume and average pore size for the adsorbents. N_2 adsorption-desorption experiments showed that AC has high surface area of $249.5 \text{ m}^2/\text{g}$. The average pore width ($L=7.14 \text{ nm}$) suggests that AC is a mesoporous adsorbent. MWCNT has lower surface area ($193.7 \text{ m}^2/\text{g}$) and pore volume (0.250 mL/g) [44] than AC, which is similar to the values reported by Li *et al.* [25]. The value of the average pore width (15.51 nm) shows that multiwalled carbon nanotubes have a mesoporous structure which may have come from the inner cavities and the agglomerations of MWCNTs. A similar phenomenon was reported by Li *et al.* [25]. Carbon nanotubes form aggregated pores due to the entanglement of tens and hundreds of individual tubes that have adhered to each other as a result of van der Waals forces of attraction. The aggregated pores have the dimensions of a mesopore or higher [25].

SEM was used to observe the surface physical morphology of the adsorbents. SEM micrographs of AC and MWCNT are shown in Figures 4 and 5.

Figure 4 shows that surface of AC containing cavities and pores of various sizes and shapes. These cavities were caused by the evaporation of the impregnated LiOH derived compound, leaving the space previously occupied by the reagent.

**Figure 4.** Scanning electron micrograph of activated carbon produced from cornelian cherry stones.

Effects of adsorbent dosage and contact time

Figure 6 presents the adsorption isotherms of the SY dye as the relationship between the amount of dye adsorbed per unit mass of a given carbonaceous

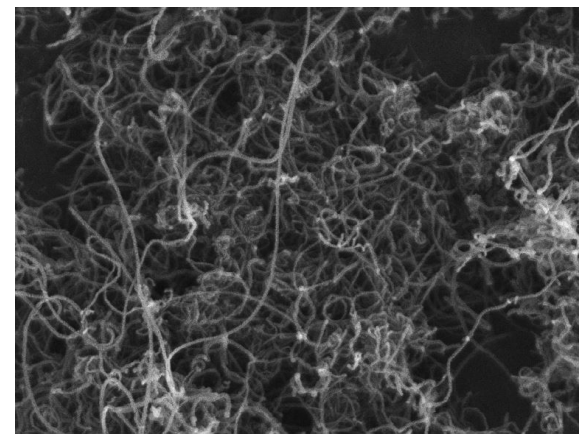
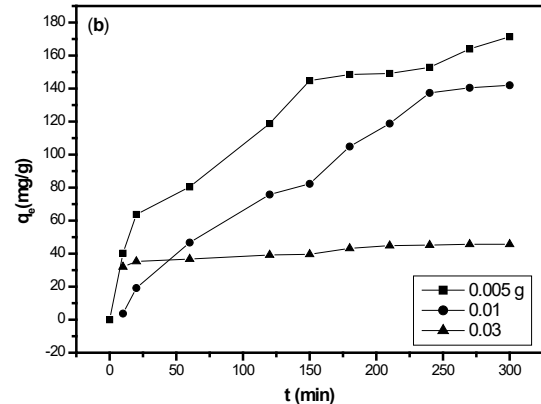
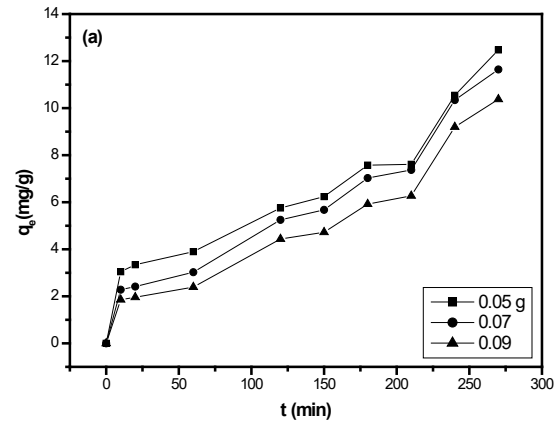
**Figure 5.** Scanning electron micrograph of MWCNT.**Figure 6.** Effects of adsorbent dosage and contact time on the adsorptive uptake of food dye onto AC (a) and MWCNT (b) (conditions: $C_0=10 \text{ mg/L}$; temperature= 40°C).

Fig. 6 (a) shows that the adsorption capacities at equilibrium (q_e) decreased with an increase in adsorbent dose from 0.05 to 0.09 g/L . Similar results have been observed for the adsorption of phenol onto activated carbon and fungal biomass [42]. In a batch of adsorption studies, the adsorption

F. O. Erdogan: Comparative study of sunset yellow dye adsorption onto cornelian cherry stones-based activated carbon and ... efficiency (E) increased from 60.43% to 90.47% when the adsorption dosage of AC increased from 0.05 to 0.09 g/L at 40 °C. This corroborates the reports of our previous study [29]. Similar behavior was reported in the literature [35, 43]. Figure 6 (b) showed that the adsorption capacities at equilibrium (q_e) decreased with an increase in adsorbent dose from 0.005 to 0.03 g/L. The adsorption capacity of MWCNT at equilibrium decreased from 171.41 to 45.02 mg/g with an increase in adsorbent dosage from 0.005 to 0.03 g/L. This is explained as a consequence of partial aggregation, which occurs at high adsorbent amount resulting in decreased active sites. Similar results have been reported for the sorption of various adsorbate onto various adsorbents in the literature [29, 34-36].

Effect of the solution temperature

The temperature dependence of sunset yellow sorption onto AC was studied at optimum adsorbent dosage of 0.05 g/L. Figure 7 shows that the food dye adsorption increased with the temperature, which may be attributed to the enhanced reaction rate at a higher temperature. The possible explanation is that a high temperature expands the pore volume and the surface area and thus provides more chances for sunset yellow dye to pass the external boundary layer and penetrate more easily. This corroborates the reports of our previous studies [27, 29]. Similar behavior has been reported in the literature [37]. The temperature dependence of SY sorption onto MWCNT was studied at optimum adsorbent dosage of 0.005 g/L. Figure 8 presents the adsorption capacity of SY dye onto MWCNT at temperatures from 30 to 50 °C. The result shows that the equilibrium adsorption capacity of SY dye decreased while increasing the solution temperature from 30 to 50 °C. The adsorption capacity of MWCNT at equilibrium decreased from 171.41 to 141.09 mg/g with an increase in the temperature from 30 to 50 °C. This decrease may be due to weakening of the bonds between the dye molecules and the active sites of MWCNT. Similar phenomena have been observed in the adsorption of remazol brilliant blue [38] and methylene blue [39] dyes onto orange peel adsorbent.

Adsorption isotherms

The equilibrium adsorption isotherms are essential to the practical design and optimization of the adsorption process. The adsorption isotherm describes how adsorbates interact with adsorbents [29]. The equilibrium data of food dye adsorption

onto adsorbents was explored using the isotherm models of Langmuir, Freundlich, Temkin and DR. The calculated parameters of the four isotherm models are and presented in Table 2.

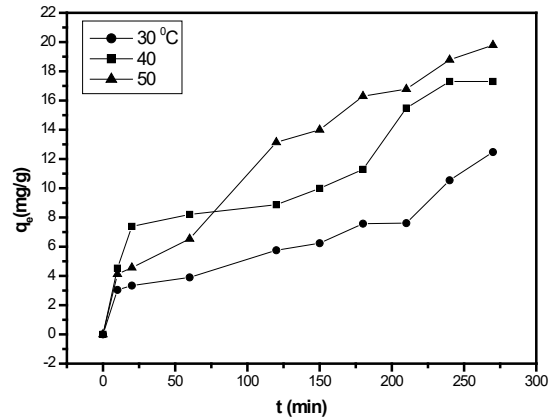


Figure 7. Effect of solution temperature on the adsorption of the food dye onto AC (conditions: W=0.05 g/L; C₀=10 mg/L).

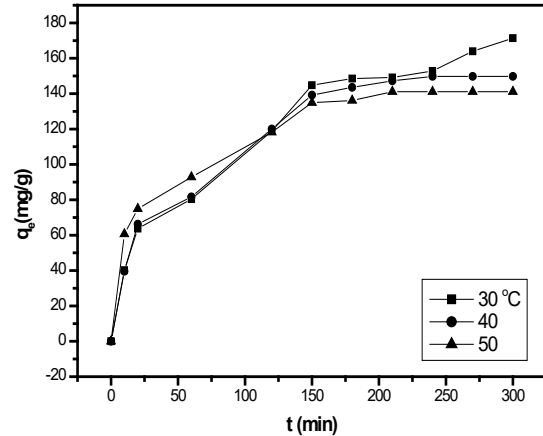


Figure 8. Effect of solution temperature on the adsorption of the food dye onto MWCNT (conditions: W=0.005 g/L; C₀=10 mg/L).

The correlation coefficients decreased in the order: DR > Langmuir > Temkin > Freundlich for AC. Langmuir adsorption isotherms constants related to adsorption capacity, Q₀, were found as 125.31 and 43.78 mg/g for AC and MWCNT, respectively. The relatively large adsorption capacity of AC could be attributed to its relatively large surface area (249.5 m²/g) and total pore volume (0.445 mL/g). The results revealed that the adsorption of food dye on AC was best described by the Langmuir isotherm, indicating the adsorption was homogeneous and a monolayer was present.

Table 2. Freundlich, Langmuir, Temkin and DR isotherm constants for the adsorption of SY dye onto AC and MWCNT at 40 °C

Isotherms		Parameters	
Freundlich	K_F (mg/g)(L/mg) $^{1/n}$	n	R^2
AC	0.4312	1.6397	0.523
MWCNT	460.29	2.291	0.453
Langmuir	Q_0 (mg/g)	K_L (L/mg)	R^2
AC	125.31	0.0087	0.905
MWCNT	43.78	0.206	0.198
Temkin	A (L/g)	b (J/mol)	R^2
AC	0.228	176.79	0.642
MWCNT	7.63E-4	-75.64	0.454
DR	q_m (mg/g)	E (J/mol)	R^2
AC	40.55	119.56	0.911
MWCNT	2199.51	325.44	0.920

Table 3. Kinetic models parameters for the adsorption of SY onto AC at different dye concentrations and temperatures.

AC		Pseudo-first order			Pseudo-second order			Elovich		
m_{ads} (g/L)	q_e (mg/g) exp	k_1 (min) $^{-1}$	q_e (mg/g)	R^2	k_2 (g/mg min)	q_e (mg/g)	R^2	β	α	R^2
10	12.475	0.0055	11.649	0.824	1.34E-3	11.541	0.765	0.435	11.534	0.696
20	25.693	0.0051	27.265	0.714	2.57E-4	26.144	0.439	0.190	57.993	0.614
30	31.374	0.0061	35.238	0.753	1.01E-4	42.265	0.331	0.136	0.5435	0.699
40	46.337	0.0062	54.141	0.720	2.05E-5	96.246	0.104	0.089	176.40	0.687
50	36.052	0.0046	39.771	0.740	3.59E-5	60.827	0.104	0.127	0.4979	0.611
T (°C)										
30	12.475	0.0055	11.649	0.824	1.34E-3	11.541	0.765	0.435	11.534	0.696
40	17.302	0.0070	15.052	0.741	1.16E-3	17.559	0.820	0.435	0.459	0.696
50	19.790	0.0104	20.944	0.932	6.33E-4	22.769	0.864	0.203	0.6895	0.901

Langmuir adsorption isotherm constant related to adsorption capacity, Q_0 was found as 125. 31 mg/g. To confirm the favorability of the adsorption, the separation factor R_L was calculated by the following equation:

$$R_L = \frac{1}{1 + K_L C_0} \quad (10)$$

where the adsorption process is either unfavorable ($R_L > 1$), linear ($R_L = 1$), favorable ($0 < R_L < 1$) or irreversible ($R_L = 0$). Here, the value of R_L was found to be 0.696 and 0.327 for AC and MWCNT, respectively, which further confirmed that the Langmuir isotherm was favorable for the adsorption of the food dye on the two adsorbents. Similar observation was reported for the adsorption of remazol brilliant blue dye on an orange peel adsorbent [38]. The value of n (from the Freundlich equation) was found to be 1.64 and 2.29 for AC and MWCNT, respectively, which is an evidence of the good adsorption of SY dye on the two adsorbents [38].

Adsorption kinetics

Adsorption kinetics provides an understanding of the mechanism of adsorption, which in turn governs the mass transfer and the equilibrium time. Sunset yellow was adsorbed on adsorbents as a function of time. Pseudo-first order and pseudo-second order and also Elovich models were obtained at temperatures of 30, 40 and 50 °C for various dye concentrations (10-50 mg/L for AC and 10-80 mg/L for MWCNT). The regression coefficients (R^2) were evaluated for all models. The results are shown in Table 3. As shown in Table 3, the highest R^2 values were obtained for the pseudo-first order kinetic model and the experimental q_e values matched well with the calculated data. It can be seen that k_1 values are increasing as the temperature increases. The higher regression coefficients indicated that the pseudo-first order model was a better fit than the pseudo-second order model.

Table 4. Kinetic models parameters for the adsorption of SY onto MWCNT at different dye concentrations and temperatures.

MWCNT		Pseudo-first order			Pseudo-second order			Elovich		
m_{ads} (g/L)	q_e (mg/g) exp	k_1 (min ⁻¹)	q_e (mg/g)	R^2	k_2 (g/mg min)	q_e (mg/g)	R^2	β	α	R^2
10	171.41	0.0101	153.50	0.963	1.37E-4	182.82	0.966	0.026	9.034	0.959
20	238.24	0.0142	79.590	0.803	9.93E-4	239.23	0.999	0.075	2254.2	0.977
50	406.56	0.0147	444.15	0.912	4.44E-5	460.83	0.902	0.039	22.436	0.855
80	130.88	0.0067	126.51	0.696	9.15E-5	136.24	0.647	0.011	5.434	0.626
T (°C)										
30	171.41	0.0101	153.50	0.963	1.37E-4	182.82	0.966	0.026	9.034	0.959
40	149.75	0.0180	154.31	0.965	2.01E-4	165.02	0.982	0.029	10.169	0.966
50	141.09	0.0174	116.95	0.953	3.69E-4	149.70	0.992	0.038	23.234	0.969

Table 5. Thermodynamic parameters for the adsorption of SY onto adsorbents.

Adsorbent	Ea (kJ/mol)	ΔH° (kJ/mol)	ΔS° (J/mol)	ΔG° (kJ/mol)		
				30 °C	40 °C	50 °C
AC	25.84	110.7	368.3	-1.07	-4.28	-8.44
MWCNT	40.20	-14.58	-48.37	0.018	0.678	0.977

Therefore, it can be said that the pseudo-second order model is not suitable to explain the adsorption process accurately. Similar results have been found in our previous study [29]. Table 3 presents the results deduced from linear plots of q_t versus $\ln t$, where β is a constant related to the extension of covered surface, and α is in relationship with chemisorption rates [30]. The Elovich constants were determined from the intercepts and slope of plots. It was noted that all β values of AC were similar. The chemisorption rates, indicated by the coefficient α , vary with dye concentration; the best value was obtained in the case of 40 mg/L dye concentration.

Kinetic parameters for the removal of sunset yellow by MWCNT are represented in Table 4. The results for the MWCNT showed good agreement with the three kinetic models, especially with the pseudo-second order kinetic model, suggesting the presence of chemisorption for MWCNT. The values for k_2 are 0.000137, 0.000201 and 0.000369 g/mg min at 30, 40 and 50 °C, respectively. Similar results have been reported for the sorption kinetics of various adsorbate onto various adsorbents in literature [27, 30, 31, 40, 41]. The Elovich model was applied to the adsorption of sunset yellow on MWCNT. It was noted that all β values of MWCNT were similar, and increased with increasing temperature. Conversely, they decreased with increasing concentration. Similar results have been reported for the sorption kinetics of basic and reactive dyes onto granular activated carbon [30]. The chemisorption rates (α), vary with dye concentration, the best value was obtained in case of 10 mg/L dye concentration. The correlation coefficients of the Elovich model for MWCNT

were also high, which indicates good linearity. From the R^2 values it may be deduced that the Elovich model can be accepted as one of the characteristics of the adsorption reaction onto MWCNT. Elovich model, initially used to express the beginning of the sorption process, long before equilibrium, can be correctly used in case of chemisorption with highly heterogeneous adsorbents [30].

Adsorption thermodynamics

The activation energy (E_a) of adsorption can be evaluated using the pseudo-first order rate and pseudo-second order constants for AC and MWCNT, respectively. The linear plot between $\ln k_1$ or $\ln k_2$ versus $1/T$ was used to calculate E_a using equation 7 and the results are given in Table 5. The E_a gives an idea about the type of adsorption process (physical or chemical). Low energies (E_a : 5-40 kJ/mol) are characteristic for physical adsorption, while higher activation energies (E_a : 40-800 kJ/mol) suggest chemical adsorption [31]. The value of E_a given in Table 5 confirms the nature of the physisorption process of SY onto AC. The E_a value was thus determined to be 40.2 kJ/mol for the second adsorption process, which indicates the chemisorption nature of SY adsorption onto the MWCNT.

The values of ΔH° and ΔS° , determined from the slope and intercept or the plot of $\ln K_C$ vs $1/T$ are reported in Table 5. The negative values of ΔG° obtained at different temperatures as seen in Table 5, show that the SY adsorption on AC was spontaneous and physical in nature, but SY adsorption on MWCNT was non-spontaneous which was revealed by the positive values of ΔG° at all temperatures under study. The increase in the

F. O. Erdogan: Comparative study of sunset yellow dye adsorption onto cornelian cherry stones-based activated carbon and ... magnitude of ΔG° with increase in temperature showed an increase in the feasibility of adsorption at higher temperatures [9, 23,24]. The positive value of both ΔH° and entropy ΔS° obtained for SY adsorption on AC showed that the adsorption process was endothermic and had random characteristics. This further confirmed the results of the studies on the effect of solution temperature on the adsorption for AC. Similar results were reported for the adsorption of disperse yellow 211 dye using low-cost adsorbents [29]. ΔH° was determined to be -14.58 kJ/mol, indicating the exothermic nature of the adsorption process for SY on MWCNT. This result is in agreement with the decrease in the equilibrium adsorption capacity with increasing temperature. The negative values of ΔS° suggest decreased randomness at the solid/solution interface and no significant changes occurring in the internal structure of the adsorbent through the adsorption of SY onto MWCNT. Similar results were reported for adsorption of basic violet 10 using MCM-41 [33].

CONCLUSIONS

The present investigation showed that biowaste cornelian cherry stones can be effectively used as a raw material for the preparation of activated carbon via chemical activation using LiOH. The BET surface area and total pore volume of the produced activated carbon were $249.5 \text{ m}^2/\text{g}$ and 0.445 mL/g , respectively. This activated carbon (AC) and commercial multiwalled carbon nanotubes (MWCNT) were used to remove sunset yellow FCF food dye (SY) from aqueous solutions at various temperatures. In batch adsorption studies, the efficiency of SY adsorption by AC or MWCNT increased with adsorbent dosage, but the equilibrium adsorption capacity decreased significantly. Adsorption capacities of SY onto AC and MWCNT were 125.3 and 43.8 mg/g, respectively. The results showed that the adsorption capacity of AC is about 2.8 times higher than that of MWCNT. The Freundlich, Langmuir, Temkin and DR isotherm models were used for the mathematical description of the adsorption of SY dye onto AC or MWCNT at various temperatures and the results suggested that the adsorption equilibrium data fitted well to the Langmuir and DR models for AC and DR model for MWCNT. The pseudo-first order, pseudo-second order and Elovich kinetic models were used to analyze the data obtained for SY adsorption onto the prepared activated carbon and MWCNT. The kinetic calculations showed that the adsorption followed the pseudo-first order model with a multi-step diffusion process for AC. These results finally

confirmed that the adsorption of SY onto AC is controlled by both physisorption and chemisorption processes. The pseudo-second order kinetic model agrees very well with the dynamic behavior for the adsorption of SY onto MWCNT at different temperatures.

Thermodynamic constants were also evaluated using equilibrium constants changing with temperature. The negative value of ΔG° indicated the spontaneity and confirmed the favorable adsorption of SY onto AC. As the temperature increased from 30 to 50 °C, the positive values of ΔH° confirmed that the process was endothermic. The positive value of ΔS° suggested the increased randomness of SY adsorption onto AC. The enthalpy change (ΔH°) for the SY adsorption onto MWCNT was -14.58 kJ/mol, which was also found to be exothermic and the adsorption capacity decreased with the increase in temperature. The ΔG° values were positive, therefore the SY adsorption onto MWCNT was non-spontaneous and the negative value of ΔS° showed the stability of the sorption process. The activation energy of the adsorption process was calculated by performing kinetic analysis at different temperatures (30-50 °C). Activation energies were 25.84 and 40.2 kJ/mol for AC and MWCNT, respectively. This study revealed that cornelian cherry stones-based activated carbon can be used as a highly efficient and economically viable adsorbent for SY dye removal from aqueous solutions.

Acknowledgements: The author acknowledges the financial support provided by Kocaeli University Scientific Research Projects Unit. (Project No: 2014/113, 2016/019 HD and 2017/57 HD).

REFERENCES

1. J. Hayashi, T. Horikawa, I. Takeda, K. Muroyama, F. N. Ani, *Carbon*, **40**, 2381 (2002).
2. B. Y. Jibril, R. S. Al-Maamari, G. Hegde, N. Al-Mandhary, O. Houache, *J. Anal. Appl. Pyrolysis*, **80**, 277 (2007).
3. H. Benaddi, T. J. Bandosz, J. Jagiello, J. A. Schwarz, J.N. Rouzaud, D. Legras, F. Bèguin, *Carbon*, **38**, 669 (2000).
4. K. Nakagawa, S. R. Mukai, K. Tamura, H. Tamon, *Chemical Engineering Research and Design*, **85**, 1331 (2007).
5. R. Ubago-Pérez, F. Carrasco-Marín, D. Fairén-Jiménez, C. Monero-Castilla, *Microporous and Mesoporous Materials*, **92**, 64 (2006).
6. P. Ariyadejwanich, W. Tanthapanichakoon, K. Nakagawa, S. R. Mukai, H. Tamon, *Carbon*, **41**, 157 (2003).
7. M. Shimada, T. Iida, K. Kawarada, Y. Chiba, T. Mamoto, T. Okayama, *J. Mater. Cycles Waste Manag.*, **6**, 111 (2004).

8. F. Oguz Erdogan, *Analytical Letters*, **49**, 1079 (2016).
9. K. Fu, Q. Yue, B. Gao, Y. Wang, Q. Li, *Colloids and Surfaces A*, **529**, 842 (2017).
10. A. Niksiar, B. Nasernejad, *Biomass and Bioenergy*, **106**, 43 (2017).
11. A. B. Fadhil, *Energy Conversion and Management*, **133**, 307 (2017).
12. N. Arena, J. Lee, R. Clift, *Journal of Cleaner Production*, **125**, 68 (2016).
13. J. M. V. Nabais, C. E. C. Laginhas, P. J. M. Carrott, M. M. L. R. Carrott, *Fuel Processing Technology*, **92**, 234 (2011).
14. A. B. Fadhil, A. I. Ahmed, H. A. Salih, *Fuel*, **187**, 435 (2017).
15. S. S. Lam, R. K. Liew, Y. M. Wong, P. N. Y. Yek, N. L. Ma, C. L. Lee, H. A. Chase, *Journal of Cleaner Production*, **162**, 1376 (2017).
16. C. A. Philip, *J. Chem. Tech. Biotechnol.*, **67**, 248 (1996).
17. J. Guo, A. C. Lua, *Microporous and Mesoporous Materials*, **32**, 111 (1999).
18. J. Hayashi, A. Kazehaya, K. Muroyama, A. P. Watkinson, *Carbon*, **38**, 1873 (2000).
19. T. Tay, S. Ucar, S. Karagöz, *Journal of Hazardous Materials*, **165**, 481 (2009).
20. T. H. Liou, *Chemical Engineering Journal*, **158**, 129 (2010).
21. R. Aravindhan, J. R. Rao, B. U. Nair, *Journal of Hazardous Materials*, **165**, 688 (2009).
22. M. F. González-Navarro, L. Giraldo, J. C. Moreno-Piraján, *Journal of Analytical and Applied Pyrolysis*, **107**, 82 (2014).
23. X. Tian, H. Ma, Z. Li, S. Yan, L. Ma, F. Yu, G. Wang, X. Guo, Y. Ma, C. Wong, *Journal of Power Sources*, **359**, 88 (2017).
24. A. S. Al-Rahbi, P. T. Williams, *Waste Management*, **49**, 188 (2016).
25. Y. Li, Q. Du, T. Liu, X. Peng, J. Wang, J. Sun, Y. Wang, S. Wu, Z. Wang, Y. Xia, L. Xia, *Chemical Engineering Research and Design*, **91**, 361 (2013).
26. Y. Yao, H. Li, J. Liu, X. Tan, J. Yu, Z. Peng, *Journal of Nanomaterials*, Art. ID 571745, (2014).
27. T. Erdogan, F. Oguz Erdogan, *Analytical Letters*, **49**, 917 (2016).
28. M. Roosta, M. Ghaedi, A. Daneshfar, S. Darafarin, R. Sahraei, M. K. Purkait, *Ultrasonics Sonochemistry*, **21**, 1441 (2014).
29. F. Oguz Erdogan, *Journal of Textiles and Engineering*, **107**, 181 (2017).
30. K. D. Belaid, S. Kacha, M. Kameche, Z. Derriche, *Journal of Environmental Chemical Engineering*, **1**, 496 (2013).
31. B. H. Hameed, A. A. Ahmad, N. Aziz, *Desalination*, **247**, 551 (2009).
32. T. Kou, Y. Wang, C. Zhang, J. Sun, Z. Zhang, *Chemical Engineering Journal*, **223**, 76 (2013).
33. L. C. Juang, C. C. Wang, C. K. Lee, *Chemosphere*, **64**, 1920 (2006).
34. C. O. Nweke, G. C. Okpokwasili, *International Journal of Biosciences*, **3**, 11 (2013).
35. Z. Huang, X. Wang, D. Yang, *Water Science and Engineering*, **8**, 226 (2015).
36. E. Rubín, P. Rodríguez, R. Herrero, M. E. Sastre de Vicente, *Journal of Chemical Technology and Biotechnology*, **81**, 1093 (2006).
37. Z. Emami, S. Azizian, *Journal of Analytical and Applied Pyrolysis*, **108**, 176 (2014).
38. M. R. Mafra, L. Igarashi-Mafra, D. R. Zuim, É. C. Vasques, M. A. Ferreira, *Brazilian Journal of Chemical Engineering*, **30**, 657 (2013).
39. P. S. Kumar, P. S. A. Fernando, R. T. Ahmed, R. Srinath, M. Priyadarshini, A. M. Vignesh, A. Thanjiappan, *Chemical Engineering Communications*, **201**, 1526 (2014).
40. M. Auta, B. H. Hameed, *Chemical Engineering Journal*, **198-199**, 219 (2012).
41. B. H. Hameed, *Journal of Hazardous Materials*, **161**, 753 (2009).
42. C. O. Nweke, G. C. Okpokwasili, *International Journal of Biosciences*, **3**, 11 (2013).
43. S. A. Kosa, G. Al-Zhrani, M. A. Salam, *Chemical Engineering Journal*, **181-182**, 159 (2012).
44. F. Oguz Erdogan, *Chemistry & Chemical Technology*, in press (2018).

СРАВНИТЕЛНО ИЗСЛЕДВАНЕ НА АДСОРБЦИЯТА НА СЪНСЕТ ЖЪЛТО БАГРИЛО ВЪРХУ АКТИВЕН ВЪГЛЕН ОТ КОСТИЛКИ НА ДРЕНКИ И ВЪРХУ ВЪГЛЕРОДНИ НАНОТРЪБИЧКИ

Ф. О. Ердоган*

*Департамент по химия и технологии за химична обработка, Професионално училище на Коджаели,
Университет на Коджаели, Коджаели, Турция*

Постъпила на 13 декември, 2017; приета на 20 юли, 2018

(Резюме)

Целта на това изследване е да се произведе евтин активен въглен от костилки на дренки (*Cornus mas L.*) и да се сравни адсорбционното му отнасяне към хранителното багрило сънсет жълто FCF (SY) с това на търговски многостенни въглеродни нанотръбички. Активният въглен от костилки на дренки (AC) и търговските многостенни въглеродни нанотръбички (MWCNT) са охарактеризирани чрез N₂ адсорбционни изотерми и SEM. Адсорбцията на хранителното багрило SY върху AC и MWCNT е детайлно изследвана. Адсорбционният тест в статични условия показва, че степента на адсорбция на багрилото зависи от неговата концентрация, времето на контакт, температурата на разтвора и количеството адсорбент. Експерименталните данни за адсорбционното равновесие са сравнени с моделите на Лангмюир, Фройндлих, Темкин и DR и са определени параметрите на изотермния модел. Максималният адсорбционен капацитет за AC и MWCNT е определен съответно като 125.3 и 43.8 mg/g. Кинетичните данни съответстват на уравнения от псевдо-първи порядък, псевдо-втори порядък и Елович. Изчислени са скоростните константи. Установени са промените в термодинамичните параметри ентальпия, ентропия и свободна енергия на Гибс. Показано е, че активният въглен, произведен от костилки на дренки, е подходящ за адсорбция на хранителното багрило SY и може да се използва като евтин и ефективен адсорбент за обработка на промишлени отпадни води.